

# Gazi University Journal of Science

http://dergipark.org.tr/gujs



# Modernization of a Low-Energy Ion Accelerator: Control System for Ion Source, Van de Graaff Generator, and Scattering Chamber

Recep BIYIK<sup>1,\*</sup> , Osman ALACAYIR<sup>2</sup>, Tamer YALCIN<sup>2</sup>

#### Highlights

- Fiber-optic control is a successful alternative for accelerator ion source parameters.
- The Van de Graaff generator is a good alternative for low-energy accelerators.
- The lifespan of older low-energy ion accelerators can be extended using modern technology

#### **Article Info**

Received:20 Dec 2024 Accepted: 7 Sep 2025

#### Keywords

Low energy ion Accelerator Optic control system Van de Graff generator Scattering chamber

#### **Abstract**

This study presents the modernization efforts for a low-energy ion accelerator (Sames J-15), originally constructed using 1970s technology, to adapt it for contemporary experimental requirements. As part of this upgrade, a new fiber-optic-based control system was developed to manage the ion source parameters, enabling precise and reliable control of critical operational values. To meet the accelerator's high-voltage requirements, a toroidal dome-shaped Van de Graaff-type generator was designed and constructed, with a target performance of up to 800 kV and  $200 \text{ }\mu\text{A}$ . In parallel, a scattering chamber and a target system were designed and integrated into the accelerator to facilitate studies in low-energy proton-induced reactions of light nuclei, including applications in nuclear astrophysics. As a result, a previously outdated ion accelerator was reconfigured and made operational for modern nuclear physics experiments. The systems developed within this project are also considered suitable for implementation in other similarly aged accelerator facilities.

### 1. INTRODUCTION

Low-energy ion accelerators are essential tools in both scientific research and industrial applications. These systems are typically used to accelerate ions to energies ranging from a few kiloelectronvolts (keV) to several megaelectronvolts (MeV), enabling investigations in nuclear physics, materials science, and medical applications [1-4]. In materials science, they enable controlled ion implantation, allowing researchers to modify surface properties, enhance hardness, and create nanostructures for advanced electronics and coatings [5]. The semiconductor industry relies heavily on these accelerators for doping silicon wafers, a critical step in manufacturing transistors and integrated circuits with ever-smaller feature sizes [6-8]. In medicine, low-energy ion beams are used in cancer therapy, particularly in targeted radiation treatments that minimize damage to surrounding healthy tissue, as well as in the production of short-lived radioisotopes for diagnostic imaging. Additionally, these accelerators play a key role in fundamental physics research, such as studying ion-solid interactions and simulating radiation effects for space applications. In nuclear astrophysics, in particular, fusion and other key reactions often occur at energies below 1 MeV, where their cross sections can only be measured reliably using such accelerators [9-13]. Low-energy accelerators are also commonly employed in fields such as fast neutron generation, ion implantation, surface modification, and radiation effects on materials [5,14-16]. Unlike high-energy accelerators, low-energy systems are more compact, consume less power, and are easier to operate, making them accessible to universities, startups, and industrial labs.

Numerous facilities around the world operate low-energy ion accelerators, many of which were originally constructed decades ago [17-22]. While their core components remain fundamentally relevant, the technological infrastructure surrounding them—such as control systems, vacuum components, and high-

<sup>&</sup>lt;sup>1</sup>Istanbul Technical University, Energy Institute, Nuclear Research Dept., 34467 Istanbul, Türkiye

<sup>&</sup>lt;sup>2</sup>Turkish Energy, Nuclear and Mineral Research Agency, Nuclear Energy Research Institute, 34303 Istanbul, Türkiye

voltage generators—often suffers from obsolescence. Consequently, modernizing these facilities is crucial to extending their operational life and enabling new experimental capabilities.

The Sames J-15 low-energy ion accelerator, located in the TENMAK Nuclear Physics Laboratory, is a linear accelerator that has served for many years in scientific research and postgraduate education [23-26]. However, the system was built using 1970s-era technology, and most of its critical components—particularly the ion source control system, power supplies, and vacuum infrastructure—had reached the end of their operational lifetimes. In its previous state, the accelerator lacked the precision, stability, and versatility required for contemporary experimental demands.

The aim of this study is to modernize and recommission the Sames J-15 low-energy ion accelerator by addressing its critical technological shortcomings. Specifically, the project focused on:

- Developing a new fiber-optic-based control system for precise and remote adjustment of ion source parameters;
- Designing and constructing a Van de Graaff-type high-voltage generator (targeting up to 800 kV, 200 μA) to serve as a stable high-voltage supply;
- Renewing the vacuum and power supply systems to improve system reliability and performance;
- Designing and integrating a new scattering chamber to support nuclear astrophysics experiments and low-energy light-nucleus reaction studies.

This work aims not only to restore the operational capabilities of the J-15 accelerator, but also to provide a replicable framework for similar modernization projects at other aging accelerator facilities.

# 2. DESCRIPTION OF THE SAMES J-15 ACCELERATOR AND ITS COMPONENTS

The Sames J-15 ion accelerator is a low-energy linear accelerator operating with a maximum accelerating voltage of 150 kV DC. It consists of three primary components: the main acceleration unit, a high-voltage generator, and a control system.

The main acceleration unit comprises the ion source (terminal), acceleration column, beam transport elements (including an electrostatic quadrupole lens, beam shutter, diaphragm, electron suppresser ring, and target), and a vacuum system (Figure 1). The ion source is composed of an osmoregulator tube, a high-frequency (100 MHz) RF excitation source, magnet coil and a concentration coil and focusing electrode. The osmoregulator tube is filled with pressurized gas—typically hydrogen, helium, or deuterium—depending on the ion species to be accelerated. A palladium rod housed within the osmoregulator expands its pores when heated, allowing the controlled passage of gas. Heating is achieved via an applied voltage in the range of 0.0–0.6V and 0.0-20A (AC). The released gas is then directed into a Pyrex or quartz ampoule tube through a narrow copper pipe, driven by the pressure difference (Figure 2). Upon the application of RF power, the hydrogen or deuterium gas inside the tube is ionized into plasma. The resulting positive ions are extracted by a +5000 V DC potential applied to the extraction electrode. Just prior to entering the acceleration column, the ions are compressed into a narrow, intense beam by the electric field generated by the focalisation ring (Figure 2).

The accelerating column is constructed by combining eleven electrodes separated by porcelain rings, with high voltage distributed across the electrodes via 10 divider resistors 150 M $\Omega$  each and 1500 M $\Omega$  total. This configuration allows for the uniform and gradual acceleration of the ion beam along the length of the column. To ensure beam focusing and stability, a quadrupole electrostatic lens is incorporated, which prevents beam divergence before it reaches the target. A beam shutter is used to block the ion beam when irradiation is not desired, while a diaphragm is positioned along the beam path to monitor the beam's diameter and spatial alignment. An electron suppressor ring is employed near the target to inhibit the backflow of secondary electrons generated upon beam–target interactions. The vacuum system supporting the beamline consists of a mechanical roughing pump with a capacity of  $10^3$  m³/s and an oil diffusion pump rated at 600 L/s [26].

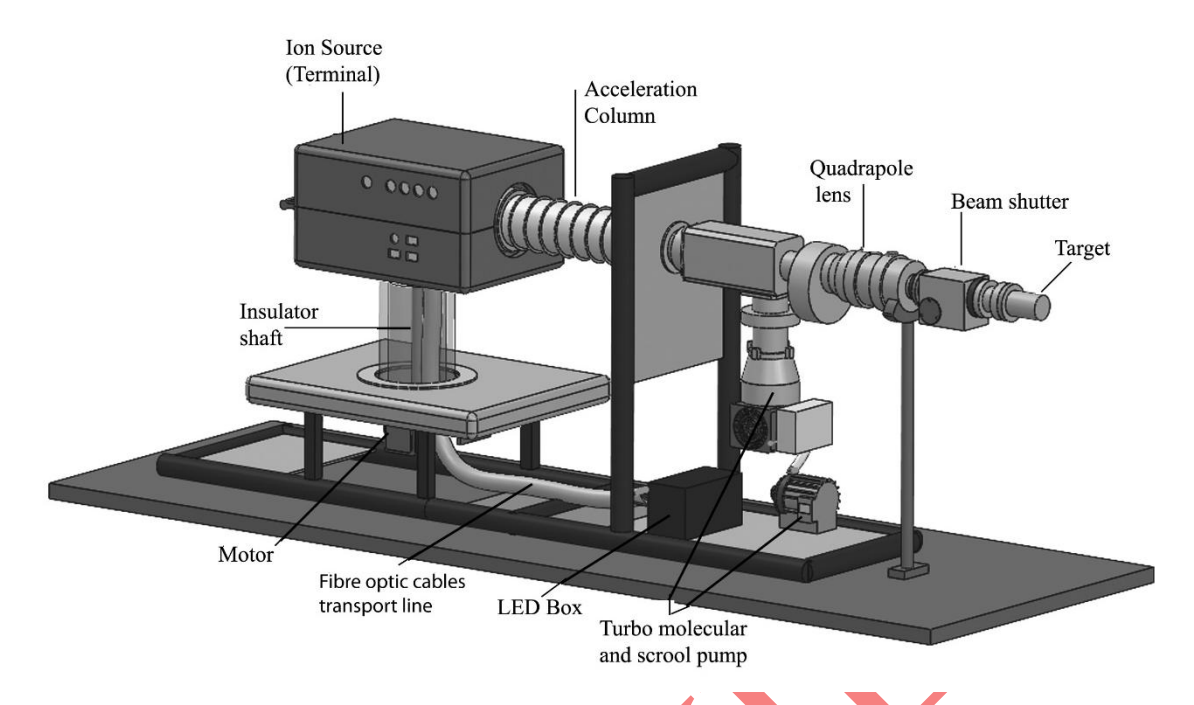


Figure 1. Low-energy Sames J-15 accelerator and components

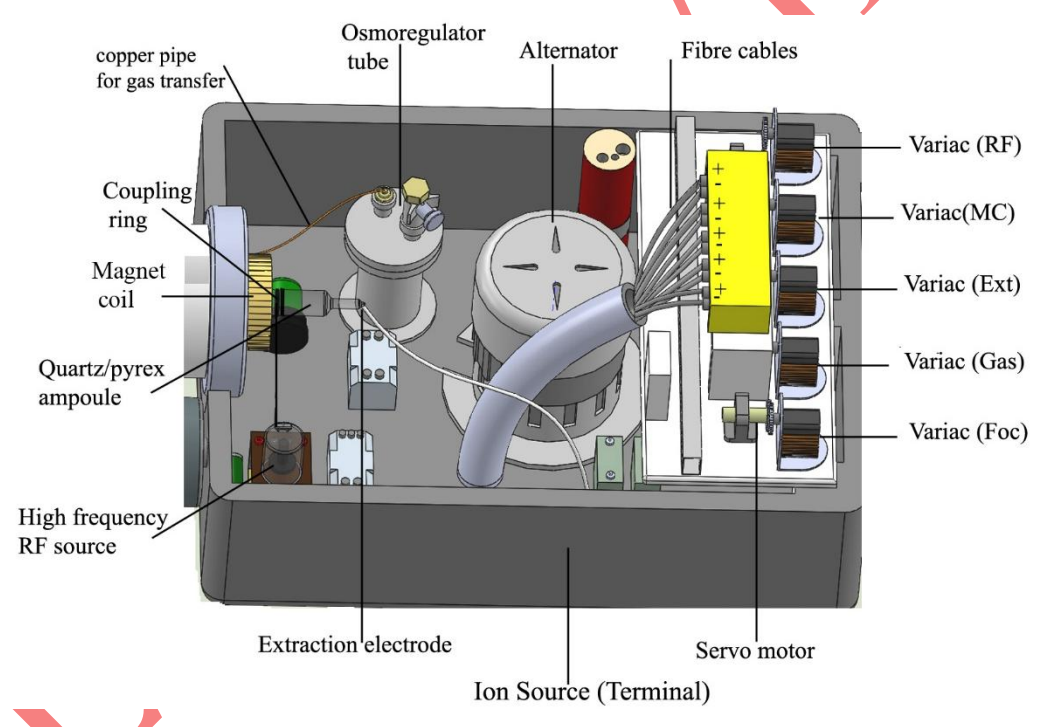


Figure 2. The ion source (terminal) section of accelerator. The alternator system drives the RF (Radio Frequency), MC (Magnet Coil), Ext. (Extraction), Gas, and Foc (Focalisation) components controlling the ion source parameters. The control system based on fiber optics is developed to control these circuits

The high-voltage unit comprises a hermetically sealed rotor-stator-type high-voltage generator and its associated power supply. The generator housing is pressurized with hydrogen gas at 15 bar to ensure insulation and discharge suppression. The power supply system includes the 30 kV excitation voltage for the generator, auxiliary low-voltage supplies, and various regulation and protection circuits designed to ensure stable and safe operation.

The control unit is equipped with a comprehensive set of indicators and interfaces that enable full remote operation and monitoring of the accelerator system. It facilitates the activation and regulation of the high-

voltage generator, precise control of the gas flow into the ion source, and adjustment of both the intensity of the RF excitation source and the focusing voltage applied to the focusing ring. In addition, the control unit provides real-time readings of key operational parameters, including high-voltage and beam current levels, vacuum level, and the current intensities measured at the target and diaphragm positions. This configuration ensures precise tuning of beam conditions and safe, efficient accelerator operation.

# 3. TECHNICAL ISSUES ENCOUNTERED IN THE SAMES J-15 ACCELERATOR AND PROPOSED SOLUTIONS

Several critical issues were identified that hindered the effective operation of the accelerator system:

- The energy required to power the ion source control components—such as the RF oscillator, focusing system, gas input control, electromagnets, and extraction system—was originally supplied via high-voltage transformers located outside the terminal, using high-voltage insulated cables. Over time, degradation of the insulation on these transformers led to voltage breakdowns and arcing, ultimately rendering the transformers inoperable.
- Persistent vacuum leaks and the inadequacy of the existing vacuum pumps prevented the establishment of the low-pressure environment necessary for reliable accelerator operation and experimental work.
- The high-voltage generator frequently malfunctioned, and due to the outdated nature of the technology, replacement parts were unavailable, making repair and consistent operation increasingly difficult.
- The absence of a scattering chamber, essential for nuclear astrophysics experiments involving reactions between accelerated particles and target nuclei, limited the accelerator's experimental utility. Such a chamber is critical for detecting reaction products and measuring cross sections in low-energy nuclear reaction studies.

Each of these issues was systematically analysed and addressed within the scope of the refurbishment project, resulting in a comprehensive modernization of the accelerator system.

### 3.1. Modifications to the Ion Source (Terminal) Section

In the ion source (terminal) section, the original transformers and high-voltage transmission cables—previously used to supply power to the ion source control mechanisms—were completely removed due to their deteriorated insulation and operational unreliability. As an alternative solution, it was proposed to generate the required power internally within the terminal by integrating an alternator-based system.

To implement this, a 220 V electric motor was mounted at the base of the terminal, and its rotational motion was transmitted to an alternator positioned within the terminal via an electrically insulated shaft (Figure 1). Coupling adapters were installed at both ends of the shaft to ensure stable and efficient mechanical transmission. The alternator's 220 V (AC) output was then stepped down to 130 V (AC)—matching the operating voltage requirements of the internal components—using a dedicated transformer. The system was installed to meet the consumption of approximately 570 W inside the terminal. This configuration enabled a reliable and safe internal power supply for the ion source control systems, eliminating the need for external high-voltage transmission lines.

A novel control system was developed to regulate five key components responsible for the ion source parameters. Each component is managed through an integrated mechanism consisting of a switch circuit, a servo motor, and a variac. The switch circuits are operated via fiber-optic signal transmission, which provides electrical isolation and minimizes interference, while the servo motors are activated by signals delivered from LED-based light sources [9, 27] (Figure 2).

Upon receiving the optical signal, the servo motors adjust the variac settings, thereby varying the output voltage between 0 and 130 V. This configuration enables fine-tuned, remote control of each ion source parameter with high precision. The complete electronic schematic of the control system is presented in Figure 3.

An additional modification implemented in the refurbishment of the J-15 accelerator involved the replacement of the existing vacuum pumps. The original vacuum system consisted of a two-stage mechanical pump and an oil diffusion pump, supported by a liquid nitrogen-assisted cold trap. Although this configuration remained operational for an extended period, it eventually reached the end of its service life and could no longer maintain the required vacuum levels.

In the upgraded system, a turbomolecular pump paired with a scroll pump was installed to achieve high-vacuum conditions more efficiently and reliably (Figure 1). Following a successful vacuum leakage test, the new system was commissioned, achieving a base pressure of  $1.6 \times 10^{-6}$  mbar, which meets the requirements for accelerator operation.

## 3.2. Design and Production of High Voltage Source (Van de Graaff Generator)

Van de Graaff generators are well-suited for low-energy nuclear experiments (typically below 2 MeV), including astrophysical studies focused on stellar nuclear reactions that require low-energy particle collisions [28]. These accelerators are capable of delivering monoenergetic ion beams with high energy resolution and stability, which are essential for precise cross-section measurements in nuclear astrophysics. Their relatively simple structure, ease of maintenance, and modularity make them a practical and cost-effective option for laboratory-scale experiments [29].

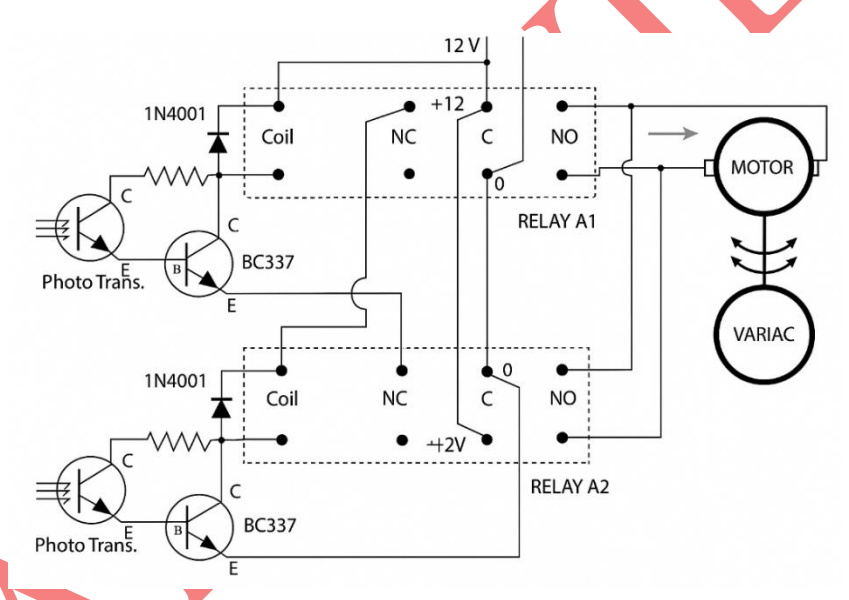


Figure 3. The electronic circuit diagram of the fiber optic control mechanism

To provide the required high-voltage source for the Sames J-15 accelerator, a Van de Graaff-type generator was designed and fabricated in-house (Figure 4). The design was guided by several key parameters, including the required output voltage and current, mechanical stability, insulation strategy, and operational compatibility with the accelerator system. The target voltage range was set based on two main considerations: (1) the Sames J-15 accelerator's maximum operational voltage limit of 150 kV, and (2) the desire for a future-proof system capable of reaching up to 800 kV for other experimental applications. A current output of up to 200 μA was targeted to meet the beam intensity needs of nuclear experiments.

The generator consists of three main components: the main body, an external charging system, and a control unit. The metal dome was designed using 68 aluminium rings, with diameters ranging from 80 to 210 cm and an internal diameter of 2 cm (Figure 4b). These rings were arranged on a toroidal Plexiglas frame to ensure structural integrity and proper electric field distribution. Plexiglas was selected for the support structure due to its excellent insulating properties, mechanical rigidity, and ease of fabrication.

The charging belt system, a crucial element of the design, consists of dual PVC belts driven by two pulleys connected to a single shaft powered by a soft-start motor. The soft-start functionality was included to protect the belt system from mechanical stress during start-up, a common issue in high-voltage charging systems.

During initial test measurements, the generator successfully produced a current of 100  $\mu A$  across a 1500 M $\Omega$  load at 150 kV (Figure 5a). The belts transport surface charge from the external charging unit—rated at 20 kV—onto the dome, generating high voltage through charge accumulation (Figure 5b). Although the maximum voltage applied to the J-15 accelerator is limited to 150 kV, the generator itself is capable of reaching voltages up to 800 kV and delivering up to 200  $\mu A$  of current, depending on experimental requirements. The control unit, designed for remote operation and fine adjustment of charging parameters, is shown in Figure 5c. At the time of writing, performance tests and calibration procedures are ongoing to validate system stability and safety under extended operation.

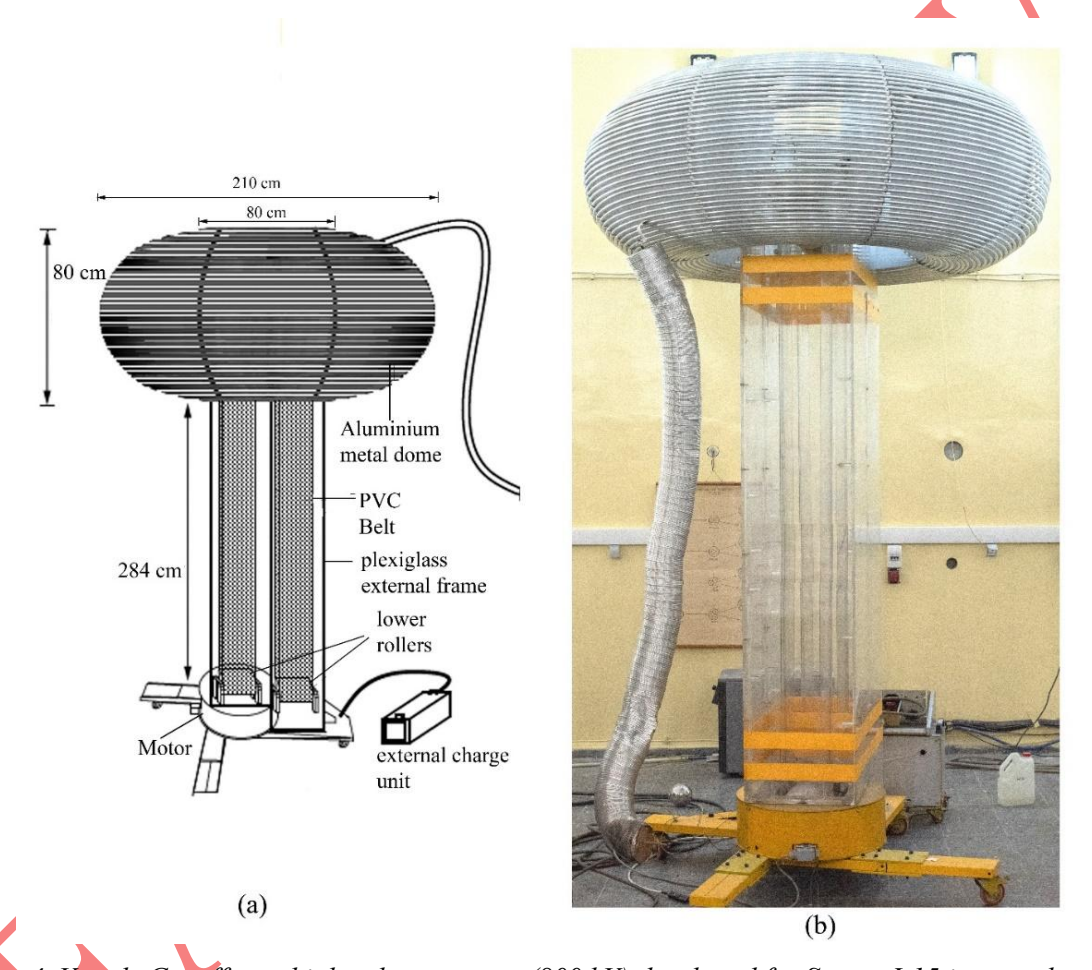


**Figure 4.** Van de Graaff type high voltage source (800 kV) developed for Sames J-15 ion accelerator (a) technical drawing image, (b) original image

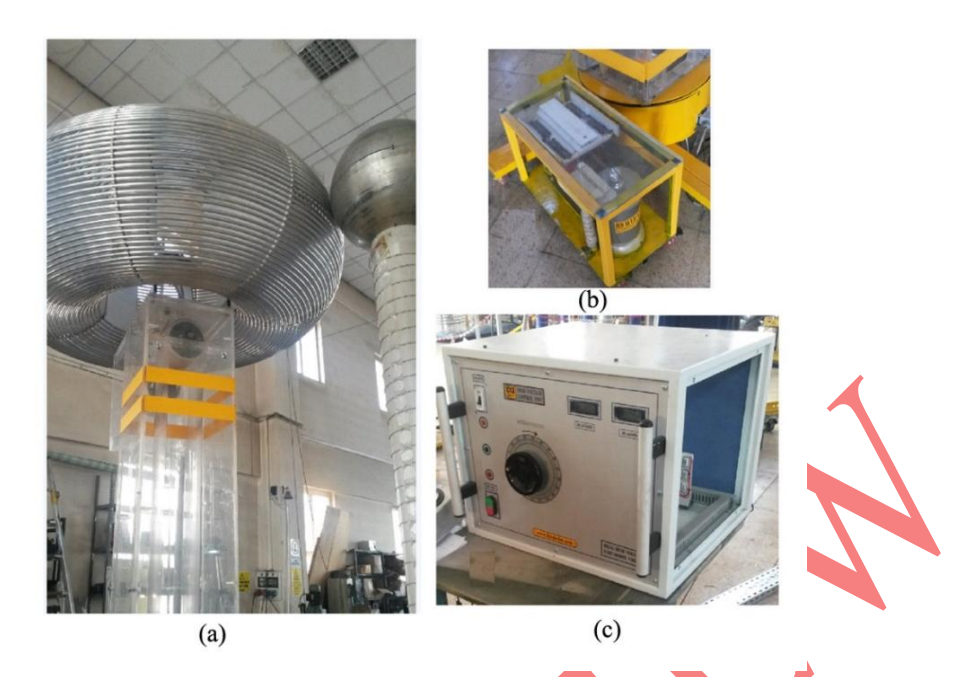


Figure 5. (a) Test measurement of the generator at 150 kV on a load resistance of 1500 MOhm (b) 20 kV external charging unit and (c) control unit of the Van de Graff generator

## 3.3. Scattering Chamber Design and Production

A scattering chamber is a critical experimental component used in low-energy nuclear physics, where accelerated particles are directed onto a target under vacuum conditions, and the resulting reaction products—particles or radiation—are detected [30]. In the design of such chambers, several functional requirements must be addressed. These include the ability to mechanically manipulate internal components externally while maintaining vacuum integrity, adjust the position of the target material, vary detector angles, accurately determine beam alignment, provide cooling for the target (if required), measure target current, and perform repetitive or sequential measurements with high precision.

Scattering chamber designs are usually designed in accordance with the experimental set-up of the researchers themselves [9,30-31]. In this study, a custom scattering chamber was designed and fabricated, primarily intended for experimental investigations in nuclear astrophysics, specifically focusing on low-energy proton-induced reactions on light nuclei. Target cooling, variable detector geometry and high-precision alignment are highlights of the scatter chamber. Nonetheless, the chamber's modular structure and versatile geometry allow it to be adapted for various other nuclear physics applications [32].

The chamber was constructed using SS304-grade stainless steel, chosen for its excellent vacuum compatibility and mechanical strength. The system was engineered to support an ultimate vacuum level of  $10^{-8}$  mbar, necessary to minimize beam scattering and maintain the purity of reaction conditions. Structurally, the chamber is cylindrical with an outer diameter of 400 mm and an internal height of 160 mm. The design incorporates one ISOK-160 flange for a viewport, eight ISOKF-40 flanges to accommodate ports for detectors, manipulators, or feedthroughs, and one ISOK-63 flange for high-vacuum pumping or additional instrumentation (Figures 6a and 6b).

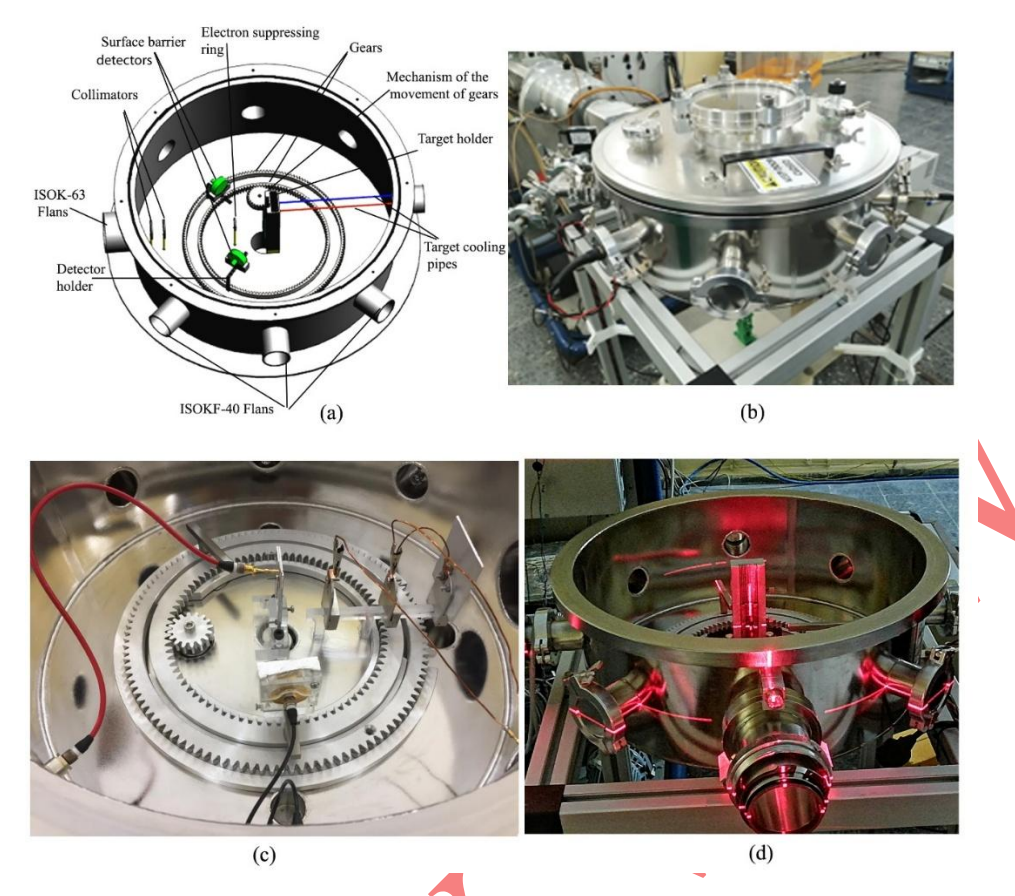


Figure 6. (a) Technical drawing of the scattering chamber and its components, (b) image of the scattering chamber mounted on the accelerator, (c) mounting of components such as surface barrier detector, detector movement mechanism gears, collimators, electron trap etc. in the scattering chamber, (d) fixing of components to the scattering chamber by laser positioning

Key components—including the target holder, beam collimators, electron suppressor ring, two surface barrier detectors, and mechanical control systems—were precisely installed inside the scattering chamber using a three-dimensional laser positioning system (Figure 6d). The electrical connections for current measurements and control were established using 9-pin and 4-pin Pfeiffer electrical feedthroughs, with signal transmission facilitated through microdot cables [27] (Figure 6c).

The beam collimators consist of 3 cm-diameter stainless steel discs featuring a 3.5 mm central aperture (Figure 6a). Mounted on a sled along the beam axis, these collimators can be moved forwards and backwards relative to the target. Their function is to ensure precise alignment of the beam to strike the target at 0° incidence, thereby minimizing angular scattering. Due to the relatively low beam current range (50–100 nA), active cooling of the collimators was deemed unnecessary.

An electron suppressor ring, positioned in the same plane as the collimators and similarly mounted on the sled, was fabricated from stainless steel. It operates under a variable negative DC voltage (0–200 V), which prevents secondary electrons—emitted from the target due to proton impacts—from escaping, thereby improving charge collection accuracy and minimising background noise.

The target holder assembly is equipped with a rotary/linear feedthrough, allowing precise angular adjustment relative to the incoming beam. It also features vertical movement capability, enabling repeated irradiation of the same target at different positions to reduce localised heating and wear. The rear of the target holder incorporates a comb-like finned design to maximize surface contact with the cooling system. While the holder is mobile, the cooler remains fixed in place. Blue and red copper tubing provides cold and hot water flow, respectively (Figure 6a), and is connected to a liquid feedthrough to maintain vacuum integrity during fluid circulation.

Following the completion of all necessary installations and system upgrades, a series of test irradiations were performed. A 0–5000 V extraction voltage was applied, and resulting beam currents were measured directly from the target via a Kapton-coated conductor routed through an electrical feedthrough. The collected signal was digitized using a digital current integrator and counted via a pulse counter. The irradiation parameters and measured current values are summarised in Table 1.

A series of test measurements were conducted to evaluate the performance of the upgraded accelerator system, including the newly developed ion source control unit, the redesigned extraction electrode, and the installed scattering chamber. During these tests, key operational parameters such as vacuum level, supply voltages, beam extraction conditions, and current readings from various components were systematically recorded (Table 1).

The measured extraction currents increased with applied voltage, reaching a maximum of 1.0 mA at 3.5 kV (Test 6). Correspondingly, target currents—which reflect the beam current incident on the target—varied from 1.5 nA (Test 4) to 600 nA (Test 8), demonstrating the system's ability to deliver a stable and controllable beam across a wide dynamic range. Collimator currents ranged from 0–22 µA, and in the case of higher extraction settings, a small current was also detected on the diaphragm (e.g., 2.5 µA in Test 7), indicating slight beam halo or misalignment.

The tests confirmed that the ion optics and focusing elements (e.g., electrostatic quadrupole lens) effectively maintained beam coherence, especially at higher extraction voltages. Notably, Test 8 provided optimal conditions with 600 nA of target current at 2.5 kV extraction, establishing a suitable configuration for future experimental applications.

The performance of the refurbished accelerator and its subsystems was evaluated against comparable systems in the literature. The designed Van de Graaff generator is capable of reaching 800 kV and producing a beam current of up to 200 µA. Although test measurements have so far been performed up to 150 kV due to insulation constraints, this current-voltage combination is consistent with standard operating parameters of high-voltage single-ended electrostatic accelerators, which typically reach 200–1000 kV and support beam currents of 100–500 µA [33]. The fiber-optic-based control mechanism for the ion source parameters represents a novel solution for low-energy accelerators, enabling electrical isolation of servo-controlled variacs through optically activated LEDs. While fiber-optic systems are used in high-power accelerator complexes for diagnostics and timing synchronization [34], their application to real-time power regulation in ion source control systems is not widely reported and therefore constitutes an important innovation in compact accelerator modernization.

Similarly, the achieved vacuum level of  $4\text{-}6\times 10^{-6}$  mbar and target beam currents up to 600 nA under extraction voltages ranging from 1.0 to 3.5 kV are within the range reported for compact accelerators operating at beam energies below 250 keV. Compact proton accelerators with extraction voltages of ~30–50 keV regularly deliver  $\mu$ A-scale beam currents under vacuum conditions of  $10^{-6}$  to  $10^{-7}$  mbar. Our system—delivering 600 nA at 2.5 kV extraction and  $7\times 10^{-6}$  mbar—therefore performs comparably within its energy regime. [35]. Furthermore, the scattering chamber developed in this study integrates advanced features such as active water-cooled target holders, vertical and rotational positioning of the target, and dual-detector geometries — offering capabilities comparable to general-purpose scattering chambers used in low-energy nuclear physics laboratories [30, 31]. The combination of these design elements demonstrates that the Sames J-15 accelerator, originally built as a fast neutron generator, has been effectively transformed into a flexible, low-energy ion beam facility. The systems developed are modular and transferable, and can serve as a reference for the modernization of similar aging accelerators in research institutions.

### 3.4. Measurement Procedure and Uncertainty Analysis

The parameters listed in Table 1 were measured using calibrated instruments integrated into the accelerator's control and diagnostic systems [36]. The vacuum level was monitored using a cold cathode vacuum gauge (Pirani + Penning type), with an accuracy of  $\pm 10\%$ . The gas supply voltage, HF/RF supply voltage, focusing voltage, magnet coil supply and extraction voltage were measured with analog voltmeters

and the HF/RF current was measured using an analog ammeter calibrated up to 500 mA. The measurement accuracies are given in Table 1.

Beam currents (extraction, diaphragm, collimator, and target) were determined using a combination of high-sensitivity digital picoammeters and current integrator circuits. The target current, representing the actual beam current hitting the target, was read using a capton-coated conductor connected to a digital current integrator, then digitised and counted via a standard digital counter module. The uncertainty in current measurements ranged from  $\pm 5\%$  at low current levels (nA) to  $\pm 2\%$  for  $\mu$ A-range signals, primarily due to fluctuations in beam stability and noise in the electronic circuitry.

Systematic uncertainties arise from RF power coupling efficiency, beam alignment, detector positioning, and temperature-dependent drift in high-voltage components. To mitigate these effects, all measurements were repeated at least three times under identical conditions, and the average values are reported in Table 1. While random fluctuations were minimal due to the stabilised power supplies, all measurements were taken under steady-state conditions after system warm-up to ensure reproducibility.

These results validate the proper integration and functionality of the newly implemented subsystems and affirm that the J-15 accelerator is now capable of supporting precision nuclear experiments requiring variable low-energy ion beams.

### 4. RESULTS

In order to reactivate the SAMES J-15 low-energy ion accelerator for nuclear physics experiments, astrophysical applications, and fast neutron generation, three fundamentally novel subsystems were designed and fabricated: a fiber-optic-based ion source control system, a high-voltage Van de Graaff generator, and a vacuum-compatible scattering chamber.

The newly developed fiber-optic control system provides precise and remote control over all five critical parameters governing plasma formation and beam extraction in the ion source. This system ensures stable and reproducible irradiation conditions, fully under operator supervision and without manual intervention in high-voltage environments.

To meet the high-voltage requirements of the accelerator, a Van de Graaff-type generator capable of stable operation at up to 800 kV was designed and constructed. However, within the scope of this study and current operational testing, the generator has been operated up to 150 kV, which is the upper limit voltage applicable to the SAMES J-15 accelerator. Extended voltage performance tests of the generator toward its 800 kV design target are ongoing and will be reported in future studies.

A new scattering chamber, fabricated from SS304 stainless steel and suitable for high vacuum (down to  $10^{-8}$  mbar), was integrated into the system. This chamber was designed to accommodate multiple detector configurations, target cooling, and precision mechanical positioning, enabling a wide range of low-energy nuclear reaction experiments, particularly proton-light nucleus reactions relevant to nuclear astrophysics. The present study offers several novel contributions: a cost-effective high-voltage source custom-built inhouse, a modular and remotely operable ion source control mechanism using fiber-optics (eliminating HV transformers and HV cables), and a scattering chamber with multi-axis target manipulation under vacuum. These developments increase operational safety, experimental flexibility, and the precision of ion beam control.

In conclusion, the integrated system developed in this study significantly enhances the capabilities of the SAMES J-15 accelerator. Moreover, the modular design principles and control strategies employed here can be adapted to other small-scale accelerator systems used in experimental nuclear physics, neutron generation, and applied ion beam technologies.

*Table 1.* Irradiation parameters and currents obtained in test studies using (0-5000 V) voltage applied to the extraction electrode

Test	Vacuum	Gas	HF/RF	HF/RF	Foc.	Magnet C.	Extraction	Quadrupole	Extraction	Extraction	Diaphragm	Collimator	Target
	(mbar)	Supply	Supply	Current	Supply	Supply	Supply	Lens (QL)	(kV)	Current	Current	Current	Current
		(V)	(V)	(mA)	(V)	(V)	(V)	(kV)		(mA)	(uA)	(uA)	(nA)
Uncertainty	(0.1)	(5)	(5)	(20)	(5)	(5)	(5)	(1)	(0.2)	(0.5)	(5)	(2)	(25)
1	6 x10 <sup>-6</sup>	70	90	250	82.5	55	55	2.5	2.5	0.5	0	10	250
2	6 x10 <sup>-6</sup>	72	90	250	82.5	55	55	2.5	2.0	0.5	0	8	230
3	6 x10 <sup>-6</sup>	70	90	240	82	55	37	1.5	1.5	0.25	0	2	30
4	6 x10 <sup>-6</sup>	70	90	240	82	55	25	1.0	1.0	0.1	0	0	1.5
5	6 x10 <sup>-6</sup>	73	90	250	80	55	60	1.5	3.0	0.75	0	4	20
6	6 x10 <sup>-6</sup>	73	95	240	80	60	70	1.5	3.5	1.0	0	1	8
7	4.5 x10 <sup>-6</sup>	73	90	250	95	60	60	1.5	2.6	0.75	2.5	22	400
8	5 x10 <sup>-6</sup>	85	90	240	85	75	55	2.0	2.5	0.8	0	22	600



#### **ACKNOWLEDGEMENTS**

This study was supported by Turkish Energy Nuclear and Mineral Agency (TENMAK) with project code A2.H4.P6. The authors would like to thank Furkan BIYIK for preparing the technical drawings used in this article.

#### CONFLICTS OF INTEREST

No conflict of interest was declared by the authors.

#### **REFERENCES**

- [1] Lorusso, A., Velardi, L., Nassisi, V., Paladini, F., Visco, A.M., Campo, N., Torrisi, L., Margarone, D., Giuffrida, L., and Raino, A., "Polymer processing by a low energy ion accelerator", Nuclear Instruments and Methods in Physics Research B, 266 (10): 2490–2493, (2008). DOI: https://doi.org/10.1016/j.nimb.2008.03.031.
- [2] Długosz-Lisiecka, M., Biegała, M. and T. Jakubowska, "Activation of medical accelerator components and radioactive waste classification based on low beam energy model Clinac 2300", Radiation Physics and Chemistry, 205: 1-8. (2023). DOI: https://doi.org/10.1016/j.radphyschem.2022.110730.
- [3] Langanke, K., Feldmeier, H., Martínez-Pinedo, G., and Neff, T., "Astrophysically important nuclear reactions", Nuclear Physics A, 1037:1-12, (2007). DOI: https://doi.org/10.1016/j.ppnp.2006.12.010.
- [4] Mondelaers, W., "Applications of low-energy accelerators", CERN Yellow Reports: Monographs, Chapter II., 14: 1757-1794, (2024), OI: https://doi.org/10.23730/CYRSP-2024.
- [5] Ynsa, M. D., Ramos, M. A., Skukan, N., Torres-Costa, V., and Jakšić, M., "Highly-focused boron implantation in diamond and imaging using the nuclear reaction <sup>11</sup>B(p, α)<sup>8</sup>Be", Nuclear Instruments and Methods in Physics Research B, 348: 174–177, (2015). DOI: https://doi.org/10.1016/j.nimb.2014.11.036.
- [6] Veselov, D. S., Voronov, Y. A., and Metel, Y. V., "Simulation of low energy ion implantation in silicon", Materials Science and Engineering, 498:1-6, (2019). DOI: https://doi.org/10.1088/1757-899X/498/1/012035.
- [7] McCamey, D. R., Francis, M., McCallum, J. C., Hamilton, A. R., Greentree, A. D., and Clark, R. G., "Donor activation and damage in Si-SiO<sub>2</sub> from low-dose, low-energy ion implantation studied via electrical transport in MOSFETs", Semiconductor Science Technology, 20(5): 363–368, (2005). DOI: https://doi.org/10.1088/0268-1242/20/5/007.
- [8] Johnson, J. C., McCallum, L., Willems, H., Beveren, V., and Gauja, E., "Deep level transient spectroscopy study for the development of ion-implanted silicon field-effect transistors for spin-dependent transport", Thin Solid Films, 518(9): 2524–2527, (2010). DOI: https://doi.org/10.1016/j.tsf.2009.09.152.
- [9] Ludwig, E. J., Black, T. C., Brune, C. R., Geist, W. H., and Karwowski, H. J., "A target chamber for the study of low-energy reactions", Nuclear Instruments and Methods in Physics Research A, 388: 37-41, (1997). DOI: https://doi.org/10.1016/S0168-9002(97)00021-1
- [10] Asgari, L., Sadeghi, H., and Khalili, H., "The astrophysical S factor of p+9Be radiative capture reaction in a potential model", New Astronomy, 108: 1-5, (2024). DOI: https://doi.org/10.1016/j.newast.2023.102178.

- [11] Csedreki, L., Gyürky, G., and Szücs, T., "Precise resonance parameter measurement in the <sup>12</sup>C(p, γ)<sup>13</sup>N astrophysically important reaction", Nuclear Physics A, 1037: 1-12, (2023). DOI: https://doi.org/10.1016/j.nuclphysa.2023.122705.
- [12] Bruno, C. G., "Experimental challenges in low-energy nuclear astrophysics," Journal of Physics: Conference Series, Institute of Physics Publishing, 1078: 1-8, (2018). DOI: https://doi.org/10.1088/1742-6596/1078/1/012007.
- [13] Kabir, A., and Nabi, J. U., "Re-examination of astrophysical S-factor of proton capture <sup>9</sup>Be(p,γ)<sup>10</sup>B in stellar matter", Nuclear Physics A, 1007: 1-10, (2021). DOI: https://doi.org/10.1016/j.nuclphysa.2020.122118.
- [14] Doupé, J. P., Litherland, A. E., Tomski, I., and Zhao, X. L., "Isobar separation at low energy in accelerator mass spectrometry", Nuclear Instruments and Methods in Physics Research B, 223-224: 323-327, (2004). DOI: https://doi.org/10.1016/j.nimb.2004.04.064.
- [15] Chamizo, E., García-León, M., Synal, H. A., Suter, M., and Wacker, D. "Determination of the <sup>240</sup>Pu/<sup>239</sup>Pu atomic ratio in soils from Palomares (Spain) by low-energy accelerator mass spectrometry", Nuclear Instruments and Methods in Physics Research B, 249: 768–771, (2006). DOI: https://doi.org/10.1016/j.nimb.2006.03.136.
- [16] Mondelaers, W., "Low-energy electron accelerators in industry and applied research", Nuclear Instruments and Methods in Physics Research B, 139: 43-50, (1998). DOI: https://doi.org/10.1016/S0168-583X(97)00944-0
- [17] Gupta, D., Aggarwal, S., Sharma, A., Kumar, S., and Chopra, S., "200 kV Ion Accelerator facility at Kurukshetra University, India", Material Letters, 308: 1-4, (2022). DOI: https://doi.org/10.1016/j.matlet.2021.131294.
- [18] Redondo-Cubero, A., Borge, M.J.G., Gordillo, N., Gutierrez, P.C., Olivares, J., Perez Casero, R., and Ynsa, M.D., "Current status and future developments of the ion beam facility at the Centre of Micro-Analysis of Materials in Madrid", The European Physical Journal Plus, 136: 1-13, (2021). DOI: https://doi.org/10.1140/epip/s13360-021-01085-9.
- [19] Reza, G., Andrade, E., Acosta, L., Gongora, B., Huerta, A., Martin Lambarri, D.J., Mas-Ruiz, J., Ortiz, M.E., Padilla, S., Solis, C. and Chaves, E., "Characterization of the new hybrid low-energy accelerator facility in Mexico", The European Physical Journal Plus, 134: 1-10, (2019). DOI: https://doi.org/10.1140/epjp/i2019-12950-1.
- [20] Rajta I., Vajda, I., Gyürky, Gy., Csedreki, L., Kiss, A.Z., Biri, S., van Oosterhout, H.A.P., Podaru, N.C., Mous, D.J.W, "Accelerator characterization of the new ion beam facility at MTA Atomki in Debrecen, Hungary", Nuclear Instruments and Methods in Physics Research Section A: Accelerators, Spectrometers, Detectors and Associated Equipment, 880: 125–130, (2018). DOI: https://doi.org/10.1016/j.nima.2017.10.073.
- [21] Roumié, M., Nsouli, B., Zahraman, K., and Reslan, A., "First accelerator based ion beam analysis facility in Lebanon: Development and applications", Nuclear Instruments and Methods in Physics Research, Section B, 219-220:389–393, (2004). DOI: https://doi.org/10.1016/j.nimb.2004.01.088.
- [22] Karadeniz, H., "Design, Construction and Results of A Low Energy DC Ion Accelerator", Uludağ University Journal of The Faculty of Engineering, 23(1): 345–352, (2018). DOI: https://doi.org/10.17482/uumfd.338184.

- [23] Adnan, B., Gökçe, T. Atilla, I.R., and Nizamettin, E. M. "Measurements of Ground, First Excited-State Energy and Width of <sup>5</sup>He via d-<sup>7</sup>Li Reaction", The Second Eurasian Conference on Nuclear Science and Its Application, Kazakhstan, 367-372, (2003).
- [24] Alaçayir, O., Baydoğan, N., Baykal, A., and Biyik, R., "Measurement of S-Factor For The <sup>11</sup>B(p, α)2α Reaction at Low Energies: Carbon Build-Up Effect", Turkish Jornal of Nuclear Science, 34(1): 1-15, (2022). [Online]. Available: http://dergipark.gov.tr/tjins
- Baysoy, D.Y., Reyhancan, İ., and Subaşı, M., "Absolute Yıeld Determination Of A 14 Mev Neutron", Journal of Engineering and Natural Sciences, 39:1–10, (2011). Available: https://sigma.yildiz.edu.tr/storage/upload/pdfs/1636094342-tr.pdf
- [26] Tarcan, G., Subaşı, M., Özbir, Y., and Baykal, A., "Installation and Operation of the Sames J-15 Low Energy Ion Accelerator At Çekmece Nuclear Research and Training Centre", Mayıs, İstanbul, 1998. Available: https://inis.iaea.org/collection/NCLCollectionStore/ Public/36/003/36003502.pdf
- [27] https://www.pfeiffer-vacuum.com/global/en/products/vacuum-chambers-components/vacuum-feedthroughs", Current feedthroughs. Accessed Jun 24,2025
- [28] Burrill, E.A., "Van de Graaff, the Man and his Accelerators", Physics Today, 20(2): 49–52, (1967). DOI: https://doi.org/10.1063/1.3034150.
- [29] Trump, J. G., Merrill, F. H., and Safford, F. J., "Van de Graaff generator for general laboratory use," Review of Scientific Instruments, 9(12): 398–403, (1938), DQI: https://doi.org/10.1063/1.1752376.
- [30] Verbruggen, R., and Mcmurray, W. R. "A 90 cm Scattering Chamber with Novel Design Features", Nuclear Instruments And Methods, 104(1):197-203, (1972). DOI: https://doi.org/10.1016/0029-554X(72)90317-5
- [31] Gunn, G.D., Schmick, T. A., Wright, L., and Fox, J. D., "A Large General Purpose Scattering Chamber", Nuclear Instruments and Methods, 113: 1–3, 1973. DOI: https://doi.org/10.1016/0029-554X(73)90471-0
- [32] Yalçın, T., Kam, E., Alaçayır, O., and Bıyık, R., "Measurement of the first Townsend coefficients in dry air", Radiation Physics and Chemistry, 222: 1-6, (2024). DOI: https://doi.org/10.1016/j.radphyschem.2024.111876.
- [33] Hinterberger, F., "Electrostatic accelerators", CAS-CERN Accelerator School: small accelerators, 95-112, (2006). DOI: https://doi.org/10.5170/CERN-2006-012.95
- [34] https://neutrons.ornl.gov/sns, "OAK Ridge National Lab.," Accessed: Jun. 24, 2025
- [35] Feuchtwanger, J., Etxebarria, V., Portilla, J., Jugo, J., Arredondo, I., Badillo, I., Asu, E., Vallis, N., Elorza, M., Alberdi, B., Enperantza, R., Ariz, I., Munoz, I., Etxebeste, U., and Hernandez, I., "New Generation Compact Linear Accelerator for Low-Current, Low-Energy Multiple Applications", Applied Sciences (Switzerland), 12(9): 1-11, (2022). DOI: https://doi.org/10.3390/app12094118.
- [36] Alaçayır, O., "Investigation of Resonance Levels and Decay Kinematics of <sup>12</sup>C Compound Nuclei Formed by p+<sup>11</sup>B Reaction Channel Using Multichannel R-Matrix Analysis Method", Doctorate thesis, Yıldız Technical University, Institute of Science, İstanbul, 19-25, (2024).